

GPS Multipath Fade Measurements to Determine L-Band Ground Reflectivity Properties[†]

Adnan Kavak, Guanghan Xu, W. J. Vogel
Electrical Engineering Research Laboratory
The University of Texas at Austin
10100 Burnet Road
Austin, TX 78758-4497

Abstract - In personal satellite communications, especially when the line-of-sight is clear, ground specular reflected signals along with direct signals are received by low gain, almost omni-directional subscriber antennas. A six-channel, C/A code processing, GPS receiver with an almost omni-directional patch antenna was used to take measurements over three types of ground to characterize 1.575 GHz specular ground reflections and ground dielectric properties. Fade measurements were taken over grass, asphalt, and lake water surfaces by placing the antenna in a vertical position at a fixed height from the ground. Electrical characteristics (conductivity and dielectric constant) of these surfaces (grass, asphalt, lake water) were obtained by matching computer simulations to the experimental results.

1. Introduction

In Earth-space communication links, reflections from land, water and obstacles combine with line-of-sight signals to produce fades that can degrade the performance of the communication link. This situation is especially important when a single strong multipath signal interferes destructively with the direct signal. In digital systems, for instance, severe inter-symbol-interference (ISI) may result, increasing the bit error rate (BER). There are, however, also cases in which a multi path signal can improve signal strength, i.e., interfere constructively. The severity of multipath fading depends on the nature and electrical characteristics of the reflecting surface [1, 2, 3], the path length, and the height and directivity of the receiving antenna.

In telecommunications systems employing low-

directivity antennas, such as in land mobile (LMSS), Global Positioning (GPS), or other wireless systems using Low Earth Orbit (LEO) satellites, reflected signals need to be taken into account. Some measurements to characterize multipath fading at L-Band (1.5 GHz) utilized Inmarsat's geostationary satellites in maritime [4, 5] and LMSS [6, 7] scenarios. These studies were performed at low elevation angles and do not fully characterize LEO constellations [8] which cover both low and high elevation angles. For the hand-held phones to be used in LEO telephone, voice and data services, multipath fading may degrade the reception significantly. Under these circumstances, most of the multipath signals are the result of ground reflected signals arriving at the receiver coherent] y or incoherent] y depending on the roughness and electrical characteristics of the surface. Coherent components are caused by a smooth surface and are called *specularly reflected* signals as opposed to incoherent components or *diffusely scattered* signals which result from relatively rough surfaces [9, 10].

To model specular reflections for systems design, the permittivity of the ground has to be known. In this paper we demonstrate that it can be measured with a GPS receiver.

2. Background: Specular Reflection and Diffuse Scattering

Signals reflected from a sufficiently smooth surface are called specularly reflected signals. They are directional, phase coherent and contributed by the central Fresnel zones on the surface near the receiver. Figure 1 shows that the total field received by the antenna is the sum of direct signal and specularly reflected signal. Here, an Earth-space link is considered. Compared to the direct component, the reflected component arrives

[†] This work was sponsored in part by National Science Foundation CAREER Program under Grant MIP-9502695, the Joint Services Electronics program under Contract F49620-95-C-0045, Office of Naval Research under Grant N00014-95-1-0638, the Jet Propulsion Laboratory under Contract JPL 956520, Southwestern Bell Technology Resources, Inc., Motorola, Inc., and Texas Instruments.

with a phase difference that is a result of the physical path length difference and the phase shift caused by the reflection. The phase shift corresponding to the difference in path length can be expressed as

$$\phi = 4\pi h \sin(\theta) / \lambda, \quad (1)$$

where h , θ , and λ are the receiving antenna height, elevation angle to the satellite, and wavelength of the transmitted signal, respectively. The reflection coefficient of a plane Earth surface is given by

$$R = \frac{\sin(\theta) - \sqrt{K}}{\sin(\theta) + \sqrt{K}}, \quad (2)$$

where $K = \eta - \cos^2\theta$ for horizontal polarization, $K = (\eta - \cos^2\theta) / \eta^2$ for vertical polarization and $\eta = \epsilon_r - j60\lambda\sigma(f)$ is the permittivity of the surface. The dielectric constant, ϵ_r , and conductivity, σ (mho/m) depend not only on the frequency of the electromagnetic wave but also on the nature of the surface, the temperature, and the moisture content. A detailed explanation about these properties of the reflecting surface can be found in [1] and the references therein. Therefore, the reflection coefficient for a smooth surface is a function of the relative dielectric constant, the conductivity, the elevation angle and the frequency of the electromagnetic wave.

The reflection coefficient of the reflecting surface also depends on the polarization of the incident field. If the electric field intensity vector is in the plane of incidence, the polarization is vertical and the reflection coefficient R_v applies, while R_h applies when the wave is polarized perpendicular to the plane of incidence. The Brewster angle θ_p is the angle at which R_v goes to zero:

$$\theta_p = \tan^{-1} \sqrt{(\eta_1 / \eta_2)}. \quad (3)$$

If medium 1 is air so that $\eta_1 = 1$, then

$$\theta_p = \tan^{-1} \sqrt{(1/\eta_2)}. \quad (4)$$

In space-Earth communications, most transmitted signals are circularly polarized to reduce ionospheric effects, namely polarization changes of the wave due to free electrons in the ionosphere (Faraday Rotation) [6]. Reflection coefficients for circularly polarized waves can be derived from

those for horizontal and vertical polarization. In general, if a circularly polarized wave is incident on the surface, the resultant reflected wave will contain a component of the original circular polarization (cp), and a component of orthogonal polarization (xp). If the elevation angle is less than the Brewster angle, the cp component predominates, whereas if the angle is greater than the Brewster angle the xp component predominates. The reflection coefficient for cp and xp components can be expressed as

$$\rho_c = (R_h + R_v) / 2 \text{ and} \quad (5)$$

$$\rho_x = (R_h - R_v) / 2. \quad (6)$$

In many practical cases the ground is not perfectly smooth. If a surface is rough, energy is scattered into various directions, reducing the magnitude of the forward reflection coefficient. The surface roughness (Rayleigh criterion) criterion can be established as

$$\Delta h \leq \frac{\lambda}{4 \sin \theta}. \quad (7)$$

The surface roughness factor (reduction factor) ρ_s for slightly rough surfaces with a random height distribution is given by

$$\rho_s = \exp[-(\Delta\phi)^2 / 2]. \quad (8)$$

Miller and Brown [11] have modified (8) to

$$\rho_s = \exp[-(\Delta\phi)^2 / 2] I_0[(\Delta\phi)^2 / 2], \quad (9)$$

where I_0 is the modified Bessel function, with a value of unity or greater.

The specular reflection coefficients R_h and R_v for a rough surface are then modified to

$$R_{hs} = \rho_h \rho_s, \quad R_{vs} = \rho_v \rho_s \quad (10), (11)$$

and the reflection coefficients for circular polarization ρ_c and ρ_x will also be reduced by the same factor ρ_s . Theoretical models were developed especially to characterize sea surface reflections including specular and diffuse components for L-Band multipath [5].

Roughness of the surface tends to decrease specular reflection components and suggests including both specular and diffuse scattering components in the total field expression. Considering all the factors (diffuse scattering, antenna gain, Earth-curvature effect, shadowing factor), the total field at the receiving antenna is:

$$\begin{aligned}
E = E_{on} &+ g_{cr}(2\theta)\rho_s FD\rho_{cd} e^{j\phi} \\
&+ g_{xr}(2\theta)\rho_s FD\rho_x e^{j\phi} \\
&+ g_{cr}(\theta_d)\rho_{cd} \\
&+ g_{xr}(\theta_d)\rho_{xd}
\end{aligned} \tag{12}$$

where

- ϕ path length difference between direct and reflected signals,
- F blockage or shallowing factor, $F=2$ maximum, usually $0.1 < F < 2$,
- D divergence factor due to Earth's curvature $0 < D \leq 1$,
- ρ_s roughness parameter ≤ 1 ,
- ρ_c, ρ_x complex reflection coefficients for cp and xp components,
- $g_{cr}(2\theta)$ antenna gain relative to direct path for cp component,
- $g_{xr}(2\theta)$ antenna gain relative to direct path for xp component,
- ρ_{cd} reflection coefficient for diffuse scatter, $= R_c \rho_d$
- $g_{cr}(\theta_d)$ antenna gain relative to that for the direct path at an angle, is average effective angle for diffuse scatter.

If we neglect the diffuse scattering component, and assume that there is no shadowing and a relatively smooth surface $D=F=1$, the normalized field intensity will fall within the values of

$$1 \pm \left[|g_{cr}(2\theta)| |\rho_{cs}| + |g_{xr}(2\theta)| |\rho_{xs}| \right] \tag{13}$$

3. Experimental Setup

A picture of the experimental setup for taking L-Band ground specular reflection measurement is shown in Figure 2. The system consists of four main units; an antenna-preamplifier unit, a GPS receiver board-set, a portable computer and a 12 volt DC power supply.

Antenna-Preamplifier Unit

The antenna-preamplifier unit consists of a 60 mm diameter low profile circularly polarized patch antenna element and preamplifier circuit which amplifies the noise-like GPS spread spectrum signal within a single unit. It is attached to a large aluminum disk acting as a ground plane and mounted on a tripod in vertical position so as to receive the direct and ground reflected signals.

Normally, when used as a location determination device, the antenna is mounted horizontally.

Receiver Board-Set

Trinible's OEM commercial SVeeSix receiver [12] is used. The signal is received through the antenna feed-line connector. The receiver has six processing channels, operating at the L1 frequency using the C/A code. It processes 6 satellite signals at a time, controls the selection of tracked satellites, and extracts position and velocity information from the 50 bps data. The complete process is performed in a 16-bit microprocessor.

Portable Computer

A portable lap-top data acquisition computer is programmed for interacting with the GPS receiver and connected to the receiver via RS-232 interface. The program monitors the health of the receiver and stores the information decoded by it. This information, i.e., time, location, satellite position (azimuth and elevation angles) and signal strength, are transmitted to the PC up to twice per second. The signal level for each monitored satellite is based on an estimate of the carrier-to-noise ratio (C/N_0) and is reported in amplitude measurement units (AMU), which can be converted to a dB scale by the approximate relation

$$P_{dB} = 20 \log \left(\frac{64 P_{AMU}}{90 \sqrt{1000}} - 100.7 \right) \tag{14}$$

Three different environments were selected for L-Band ground reflection measurements: a) a grass field at the research campus of The University of Texas at Austin, b) an asphalt parking lot at the Texas Department of Human Services, and c) Lake Travis.

Table 1: Summary of GPS Ground Specular Reflection Measurements Details

Environment	antenna azimuth	satellite PRN	surface characteristics
grass	90°	23	dry, flat, clear LOS
asphalt	105°	23	dry, flat, clear LOS
water	315°	14	waves, clear LOS

4. Experimental and Simulation Results

In this section, we present experimental and computer simulation results obtained for the three locations. The most pertinent details of the experiments have been summarized in Table 1. For each case, the results are presented with three figures:

1. Measurement Results: GPS Satellite Position Change (PRN which is ID of the selected GPS satellite in the constellation, azimuth and elevation angles) and the received power variation.
2. Simulation and measurement results for the received power variation at 1.575 GHz due to direct and ground reflected signals.
3. Magnitude and phase of the estimated ground reflection coefficients for vertical and horizontal polarization.

In the simulation, (13) was used to characterize the total power fluctuation of the signal. As relatively flat measurement environments without blockage and shadowing effects were selected, the diffuse scattering component was assumed to be zero, and F and I set to 1. Signal power levels in both measurement and simulation results have been normalized to maximum signal levels. The data was collected for approximately 50-60 minutes in order to characterize the effect of the ground reflection for long-term variation relative to the 2-samples per second data rate recorded by the portable computer. Power levels recorded in AMU have been converted into dB scale as described in [12].

Figure 3 illustrates the measurement results on the grassy field. Satellite PRN 23 was chosen among the available GPS satellites of the constellation, as it had the best position that avoided shadowing and blockage. The elevation angle decreased from 25° to 6°. On the other hand, the azimuth angle increased from 110° to 130°. Both angles varied nearly linearly with respect to the 50 minute observation time interval. The observed fluctuations of the power level were almost periodic and the peak-to-peak variation was around 20 dB. This behavior was caused by the path length difference and change in the complex reflection coefficient, both of which depend on the elevation angle.

Deep fades occurred at around 1500th and 2500th seconds epoch time. Small irregularities on the grass resulted in short-term, random fluctuations imposed on the long-term variation of the signal level. However, the short-term changes do not mask the specular characteristics of the environment. Both experimental and simulation results of the received GPS signal power for the grass field are shown in Figure 4. The power levels were matched closest for conductivity $\sigma=0.08$ mho/m and dielectric constants $\epsilon_r=3.8$. Magnitude and phase characteristics of the complex reflection coefficients of dry grass at L-Band are given in Figure 6 for vertically and horizontally polarized fields. The estimated parameters, σ and ϵ_r are used in determining these coefficients. As expected, the phase of the reflection coefficient for horizontal polarization is 180°. The phase for the vertical polarization, however, shifts from -140° to -180°. The magnitude of both coefficients increases as the elevation angle decreases.

The measurement results for the asphalt covered ground arc presented in Figure 5. The same GPS satellite (PRN 23) was tracked as in the grass field measurement. Again, data was recorded for approximately 50 minutes. Similar changes in azimuth and elevation angle of the satellite were observed. The minimum fade level in the received power level, in this case, was around -15 dB and occurred at the 25001st second epoch time. As compared to the grass field (Figure 3), scattering caused higher short-term fluctuations.

Figure 7 compares simulated and measured GPS signals. A good fit is achieved with $\sigma=0.03$ and $\epsilon_r=1.5$. Specularly reflected signals from the asphalt pavement caused shallower fading than those from the grassy field. The reflection coefficient of the asphalt ground for vertical and horizontal polarization cases is plotted in Figure 8. In this case, the phase of both coefficients was almost 180° and their magnitude increased with decreasing elevation angle.

The relevant measurement results for the lake are given in Figure 10. Compared to the results for the grass and asphalt, we observed more diffuse scattering components, most likely because of the waves. The deepest null was limited to the level of -8 dB, implying lower specular signals. The selected satellite was PRN 14. Its position change

in azimuth followed non-linear variation with respect to the observation time unlike those in the grass and the asphalt measurements. The azimuth angle decreased from 318° to 296° and the elevation angle increased from 36° to 58°. The comparison of simulation and measurement results for the power variation due to the reflection from the lake are presented in Fig 10. The simulation results are matched to the experimental results by setting the parameters $\sigma=0.018$ and $\epsilon_r=2.1$, respectively. The reflection coefficients of the lake water are shown in Fig 11. The magnitude of the horizontal polarization decreased while that of the vertical polarization increased. The phase of the horizontal polarization was 180° for all values of the observed elevation angle..

Conclusions

In this paper, the effect of ground reflected L-Band signals on the received power level in satellite communication systems has been studied. The GPS system was used for making constitutive parameter measurements of a grass field, an asphalt parking lot, and lake water. Received power variations caused by the interference of direct and ground reflected signals were analyzed. In the experiments, the most favorable GPS satellite's signal among six satellites during the measurement time interval (50-60 minutes) was picked and recorded while the elevation and azimuth angle of the satellite changed. Computer simulations modeled the power variations. By matching simulated results to experimental results, conductivity and dielectric constants of the ground (grass, asphalt, and lake water) have been derived, presenting a novel way of estimating ground electrical characteristics at 1.5 GHz. If the peak-to-peak fluctuations of the normalized power (P) level are considered, the following conclusion can be made:

$$P_{\text{lake}} < P_{\text{asphalt}} < P_{\text{grass}} \quad (15)$$

We expected that the peak-to-peak fluctuation caused by the lake would be the greater because water has a large relative dielectric constant near 70. Besides making the lake measurement at a higher elevation angle, the surface was also quite wavy. The waves probably diffused the energy of the incident wave and yielded less specular reflection.

Bibliography

- [1] ITU. "Electrical Characteristics of the Surface of the Earth," *Propagation in Non-Ionized Media*, Report 729-6, 1990 Annex to Vol. V
- [2] ITU, "Methods for Estimating Effective Electrical Characteristics of the Surface of the Earth," *Propagation in Non-Ionized Media*, Report 879-1, 1990 Annex to Vol. V
- [3] ITU, "Reflection from the Surface of the Earth," *Propagation in Non-ionized Media*, Report 1008-1, 1990 Annex to Vol. V
- [4] D. J. Fang, F.-T. Tseng and T. O. Calvit, "A Low Elevation Angle Propagation Measurement of 1.5 GHz Satellite Signals in the Gulf of Mexico," *IEEE Trans. on Ant. and Prop.*, Vol. 30, No. 1, Jan. 1982
- [5] Y. Karasawa and I. Shiokawa, "Characteristics of L-Band Multipath Fading due to Sea Surface Reflection," *IEEE Trans. on Ant. and Prop.*, Vol. 32, No. 6, pp. 618-623, Jun. 1984
- [6] J. Goldhirsh and W. J. Vogel, *Propagation Effects for Land Mobile Satellite Systems: Overview of Experimental and Modeling Results*, NASA Reference Publication 1274, Feb. 1992
- [7] W. J. Vogel and J. Goldhirsh, "Multipath Fading at L Band for Low Elevation Angle, Land Mobile Satellite. Scenarios," *IEEE J. Select. Areas in Comm.*, Vol. 13, No. 2, pp. 197-204, Feb. 1995
- [8] R. J. Leopold and A. Miller, "The Iridium Communications System," *IEEE MTT-S Digest*, pp. 575-578, 1993
- [9] P. Beckmann and A. Spicichino, *Scattering of Electromagnetic Waves from Rough Surfaces*, Pergamon Press, Oxford, UK, 1963
- [10] J. R. Wait, *Electromagnetic Waves in Stratified Media*, Pergamon Press Inc., New York, 1962
- [11] A. R. Miller, R. W. Brown and E. Vegh, "New Derivation for the Rough-Surface Reflection Coefficient and for the Distribution of Sea-Wave Elevations," *IEEE Proc.*, Vol. 131, pp. 114-116, April 1984
- [12] *Trimble Standard Interface Protocol Toolkit User's Manual*, Trimble Navigation Inc., Jun. 1993

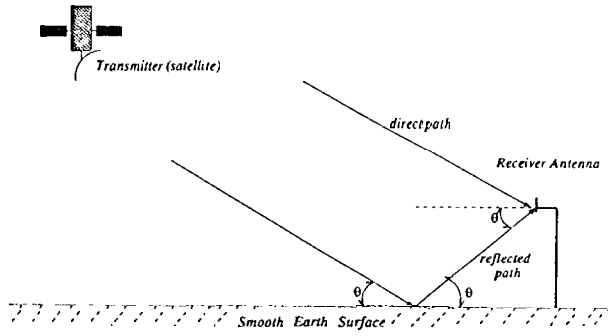


Figure 1: Specular Reflection Model



Figure 2: Experimental Setup for L-Band Specular Reflection Measurement

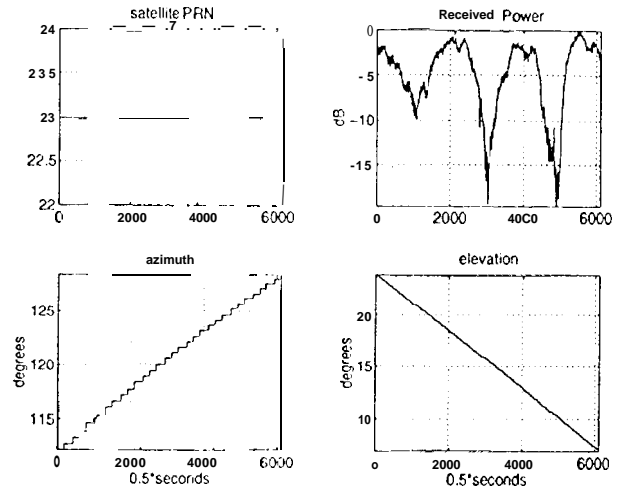


Figure 3: Grassy Field GPS Measurement Details

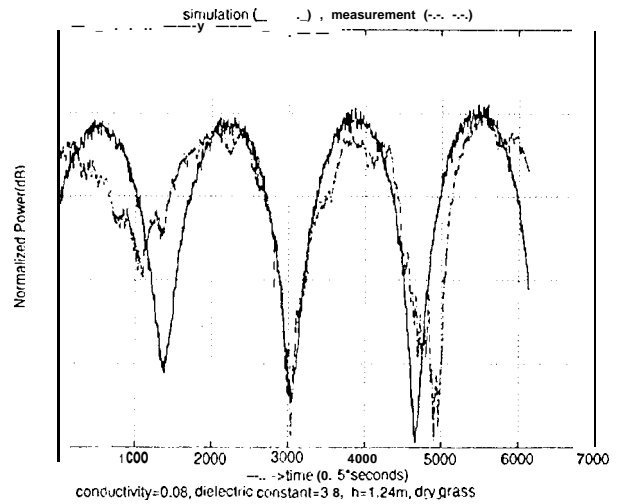


Figure 4: Modeled and Measured Signal Variations Received on a Dry Grass Field

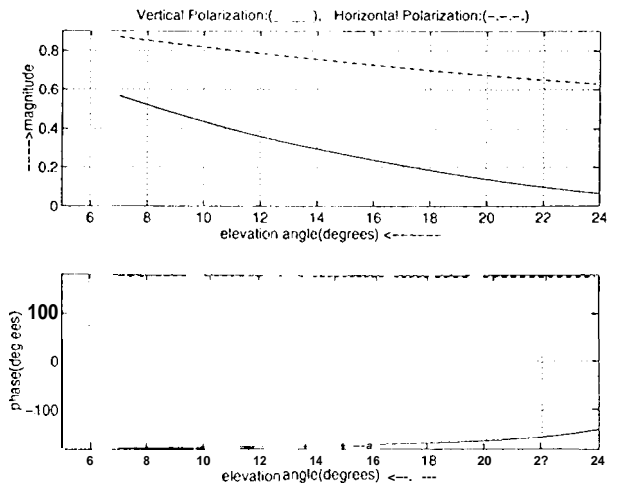


Figure 5: Reflection Coefficients for Dry Grass at 1.575 GHz

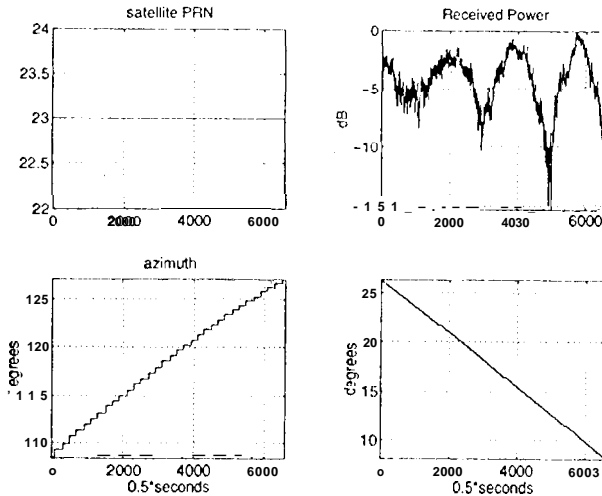


Figure 6: Asphalt Pavement GPS Measurement Details

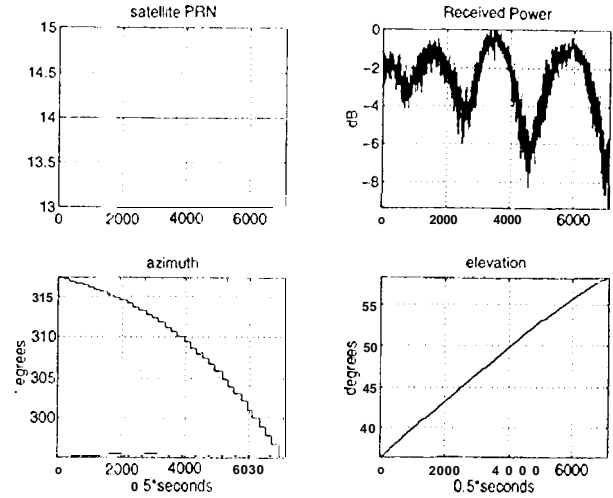


Figure 9: Lake Water GPS Measurement Details

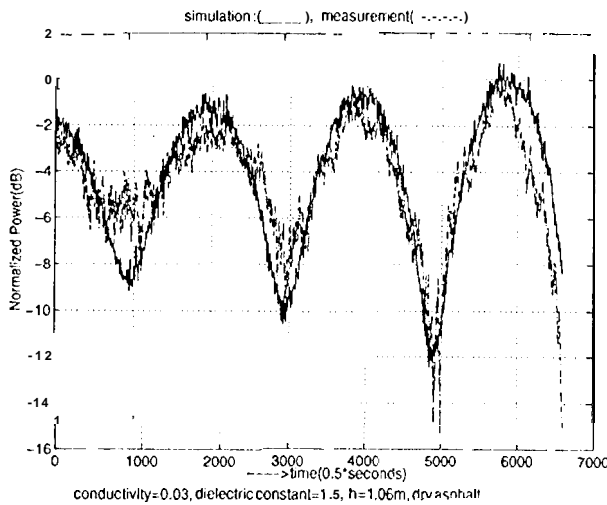


Figure 7: Modeled and Measured Signal Variations Received on an Asphalt Parking Lot

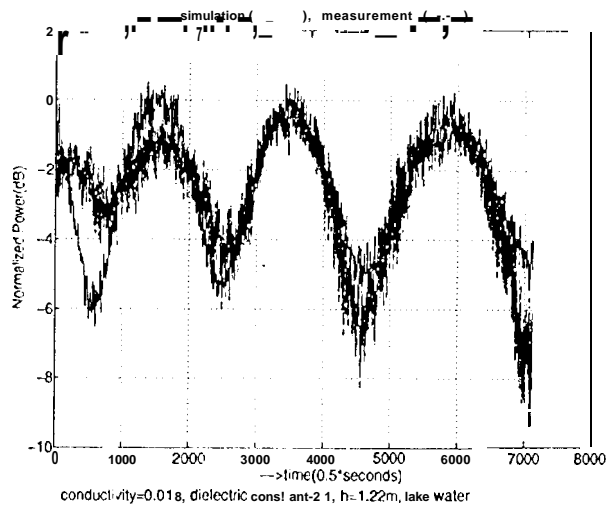


Figure 10: Modeled and Measured Signal Variations Received Over Water at the Lake

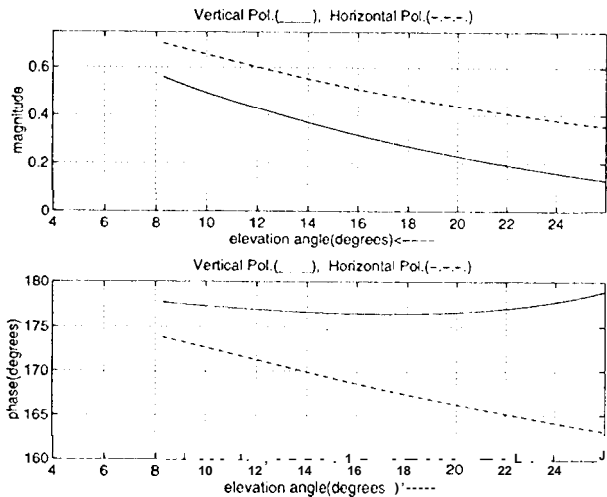


Figure 8: Reflection Coefficients for Dry Asphalt Pavement at 1.575 GHz

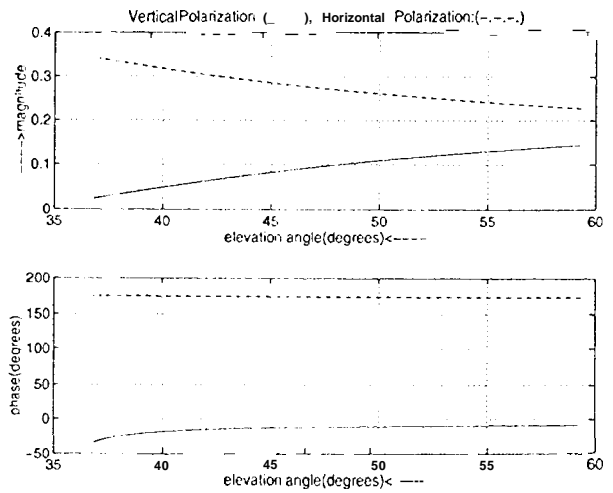


Figure 11: Reflection Coefficients for Lake Water at 1.575 GHz